NASA Contractor Report 172274

NASA-CR-172274
19840007829

ICASE

ACOUSTIC SHOCKS IN A VARIABLE AREA DUCT CONTAINING NEAR SONIC FLOWS

S. I. Hariharan

and

Harold C. Lester

Contract Nos. NAS1-17070, NAS1-17130
December 1983

INSTITUTE FOR COMPUTER APPLICATIONS IN SCIENCE AND ENGINEERING
NASA Langley Research Center, Hampton, Virginia 23665

Operated by the Universities Space Research Association

NASA
National Aeronautics and
Space Administration
Langley Research Center
Hampton, Virginia 23665

Acoustic Shocks in a Variable Area Duct Containing Near Sonic Flows

by

S.I. Hariharan

University of Tennessee Space Institute

Tullahoma, TN 37388

and

Institute for Computer Applications in Science and Engineering

Harold C. Lester

NASA Langley Reserch Center

Hampton VA 23665

ABSTRACT

In this paper we consider acoustic shock waves in a variable area duct which contains near sonic flows. The problem we treat here is modelled after an aeroengine inlet. It is known experimentally that area variation of a duct and high Mach number mean flow can reduce acoustical energy yielding substantial noise reduction. One possible reason for this is acoustic shocks. We describe the use of an explicit numerical method which is very accurate and also captures shocks reasonably well. Comparisons of the results are made with an existing asymptotic theory for Mach numbers close to unity. When shock occurs reduction of sound pressure levels are shown by examples.

Research for the first author was supported by the National Aeronautics and Space Administration under NASA contract Nos. NAS1-17070 and NAS1-17130 while he was in residence at ICASE, NASA Langley Research Center, Hampton, VA 23665.

1. Introduction

Recently a numerical solution for the propagation of sound in a variable area duct which contains a high Mach number subsonic flow was studied by the authors (reference 4). The nature of the wave propagation was nonlinear. This note is a continuation of this work and presents some results concerning computation of shocked waves in this situation. The model problem studied here and in reference 4 serves the purpose for the study of an aero-engine inlet. Briefly there is a flow in a variable area duct and acoustic waves propagate upstream of this flow. The acoustic waves are generated by an incident plane wave on the left of the duct and leave the right end without reflecting. It was first observed experimentally (reference 3) that with a given flow and a proper choice of area variation it is possible to attenuate the sound intensity as much as 20db. Theoretical reasons for this mechanism of reduction of noise level are still under investigation. They are complicated by the fluid equations which are the Navier-Stokes equations. However, in the inviscid limit it is believed (reference 7, 8) that acoustic shocks which result in energy loss is one such possibility. Though sound level attenuation was not shown in ref. 7, they did show energy loss when shocks occur. The work in reference 7 is based on an asymptotic theory and valid for Mach numbers close to unity. In a later experimental study (reference 5) it was shown that even for Mach numbers far less than unity (about 0.7) one still obtains substantial sound reduction. Thus a numerical study was undertaken to calculate solutions for all Mach numbers.

There has been only a little published in the literature for this flow configuration. The classical Fubini solution uses an asymptotic expansion

to obtain an approximate solution to the one dimensional gas dynamic equation for a uniform duct. Polyakova (reference 10) made extensions for problems with flow and Blackstock (reference 1) for the case of shocks. For variable area ducts Myers and Callegharí (reference 8) used the method of matched asymptotic expansions. This reference was the only source for any constructive shock solution in the literature. Recently parallel to our work Walkington and Eversman (reference 12) carried out computations of this situation. Our study yields similar results, but we believe, our approach is simpler for the reasons indicated in the next section. Moreover the scheme used here is more accurate than the one in reference 12. The authors would like to point out that there has been other work namely Nayfeh. et al (reference 9) to compute the nonlinear, but unshocked solutions for this type of configuration.

In this work we describe the model briefly and indicate the assembly of the numerical method. We emphasize the approach we took for obtaining boundary conditions. We present numerical results obtained for shock cases and compare with the asymptotic results of reference 7. We also present noise level distribution over the duct and demonstrate the noise reduction in the situation of a shock.

2. Equations of motion

The total flow field is governed by the inviscid, compressible Euler equations. They consist of equations for continuity, momentum and energy. The energy equation can be replaced by isentropic relations provided one is seeking only weak shocks. This is exactly the case in acoustics where only weak shocks are the central goal. Strong shocks

cause disturbances in the main stream and the meaning of acoustics will not be valid. This philosophy was adapted in reference 4 and it yielded a system of two equations for acoustic density and velocity rather than three equations thus reducing computational costs.

The situation which is of interest here assumes a quasi one dimensional flow. The flow configuration is depicted in figure 1. In this a steady flow is moving from the left to right and the acoustic waves are propagating up-stream of the flow from a harmonically varying source (plane wave). Then the total field is governed by the following equations, where A(x) is the area variation of the duct:

$$\frac{\partial \overline{\rho}}{\partial t} + \frac{\partial}{\partial x}(\overline{\rho}\ \overline{u}) + \frac{\overline{\rho}\ \overline{u}}{A}\frac{dA}{dx} = 0 \tag{2.1}$$

$$\frac{\partial \overline{u}}{\partial t} + \frac{\partial}{\partial x}\left(\frac{\overline{u}^2}{2} + \frac{\gamma}{\gamma - 1}\frac{p_0}{\rho_0^{\gamma}}\overline{\rho}^{\gamma-1}\right) = 0 \tag{2.2}$$

and the pressure is determined from

$$\overline{p} = \frac{p_0}{\rho_0^{\gamma}}\overline{\rho}^{\gamma} \tag{2.3}$$

Here $\overline{\rho}, \overline{u}$ and $\overline{p}$ are the total density, velocity and pressure, respectively, and the quantities with subscript zero denote ambient values. We divide these flow quantities into 'mean' and 'acoustic' parts. That is, if mean flow quantities are assigned a subscript s then:

$$\begin{aligned} \overline{u} &= u_s + u \\ \overline{\rho} &= \rho_s + \rho \\ \overline{p} &= p_s + p \end{aligned} \tag{2.4}$$

The mean flow is assumed to be steady and they satisfy the following steady state flow equations:

$$\frac{\partial}{\partial x}(u_s\rho_s) + \frac{\rho_s u_s}{A}\frac{dA}{dx} = 0 \tag{2.5}$$

$$\frac{\partial}{\partial x}\left(\frac{u_s^2}{2}+\frac{\gamma}{\gamma-1}\frac{p_0}{\rho_0^\gamma}\rho_s^{\gamma-1}\right)=0 \tag{2.6}$$

$$p_s=\frac{p_0}{\rho_0^\gamma}\rho_s^\gamma \tag{2.7}$$

Then equations (2.1) - (2.3) yield the following nondimensional acoustic equations.

$$\rho_t+(u_s\rho+\rho_s u+u\rho)_x+(u_s\rho+\rho_s u+u\rho)\frac{1}{A}\frac{dA}{dx}=0 \tag{2.8}$$

$$u_t+\left[u_s u+\frac{u^2}{2}+c_s^2\left(\rho/\rho_s+\frac{\gamma-2}{2}(\rho/\rho_s)^2\right)\right]_x=0 \tag{2.9}$$

$$p=c_s^2\left(1+\frac{\gamma-1}{2}\rho/\rho_s\right)\rho \tag{2.10}$$

Here c_s is the local sound speed in the flow and is given by

$$c_s^2=\gamma\frac{p_s}{\rho_s} \tag{2.11}$$

The details of derivation of these equations are available in reference 4. Note that in these equations density, velocity are scaled by their ambient values ρ_0, C_0 , the pressure is scaled by $\rho_0 C_0^2$ and the area by the throat area A_t of the duct. Moreover the distance and time are scaled by $\frac{\omega}{c_0}$ and by ω , where ω is the frequency of the source. This frequency corresponds to the engine noise source. In this nondimensionalization process the meanflow speed becomes the Mach number distribution and the solution space becomes the interval [0,L], where L is the duct length multiplied by $\frac{\omega}{C_0}$.

These equations are to be solved subject to the following boundary conditions. At x = 0,

$$u(0,t)=f(t)\ \ (t>0). \tag{2.12}$$

At x = L,

$$B(u, \rho)(L, t) = 0 \tag{2.13}$$

where f(t) is the source variation and (2.13) dictates a nonreflective (impedance type) condition. We shall derive this condition in section 4.

3. Numerical scheme

We shall briefly indicate the numerical method used in this work. This method is an extended version of MacCormack's method with fourth order accuracy in space and second order accuracy in time (see reference 2). However, it should be viewed as a fourth order accurate scheme, since we are interested in steady time averaged quantities. Let the spatial discretization of the axis of the duct be given by $x_j =$
$(j-1)L/J \quad (j = 1, ..., J)$. Let us define forward and backward flux difference operators by

$$P_j^{\pm}(f) = 7f_j - 8f_{j\pm1} + f_{j\pm2} \tag{3.1}$$

Here the plus 'sign' denotes forward and 'minus' sign denotes backward operations, respectively. Then for a single equation of the form

$$u_t + f_x = h \tag{3.2}$$

the scheme works as follows:

$$\begin{aligned} u_j^{(1)} &= u_j^n - \frac{\Delta t/2}{6\Delta x} P_j^-(f^n) + \frac{\Delta t}{2} h_j^n \\ u_j^{n+1/2} &= \frac{1}{2}\left[u_j^n + u_j^{(1)} + \frac{\Delta t/2}{6\Delta x} P_j^+(f^{(1)}) + \frac{\Delta t}{2} h_j^{(1)}\right] \end{aligned} \tag{3.3}$$

This has a backward predictor and a forward corrector. In the next $\Delta t/2$ time step it is changed into a forward predictor and a backward corrector as follows:

$$\begin{aligned} u_j^{(1)} &= u_j^{n+1/2} + \frac{\Delta t/2}{6\Delta x} P_j^+\left(f^{n+1/2}\right) + \frac{\Delta t}{2} h^{n+1/2} \\ u_j^{n+1} &= \frac{1}{2}\left[u_j^{n+1/2} + u_j^{(1)} - \frac{\Delta t/2}{6\Delta x} P_j^-\left(f^{(1)}\right) + \frac{\Delta t}{2} h^{(1)}\right] \end{aligned} \tag{3.4}$$

In these formulas subscript $n, n+1/2$ and $n+1$ denote quantities evaluated at times $n\Delta t, (n+1/2)\Delta t$ and $(n+1)\Delta t$ and the superscript (1) denotes the predicted values. It is pointed out in reference 9 that alternating formulas (3.4) and (3.5) at each time step is necessary to achieve fourth order accuracy for nonlinear problems.

We note in (3.3) and (3.4) the flux difference operator P^+ is not defined for j = J-1 and j=J and P^- is not defined for j=1 and j=0. At these points fluxes are extrapolated according to the following third order formula.

$$f_j = 4f_{j+1} - 6f_{j+2} + 4f_{j+3} - f_{j+4} \quad (j = 0, -1) \tag{3.5}$$

$$f_{j+1} = 4f_j - 6f_{j-1} + 4f_{j-2} - f_{j-3} \quad (j = J, J+1) \tag{3.6}$$

When these extrapolations are applied to define the fluxes then the steps (3.3) and (3.4) are valid for all grid points j=1 through J.

This process is then applied to equation (2.8) with

$$\rho = u$$

$$f = u_s\rho + \rho_s u + u\rho$$

and

$$h = -(u_s\rho + \rho_s u + u\rho)\frac{1}{A}\frac{dA}{dx}$$

and to (2.9) with

$$u = u$$

$$f = u_s u + \frac{u^2}{2} + c_s^2\left(\rho/\rho s + \frac{\gamma - 2}{2}(\rho/\rho_s)^2\right)$$

and $h = 0$.

Artificial viscosity

Similar to fluid dynamic calculations, in order to capture shock waves without oscillations, viscous damping terms are added to the difference equations. The previous numerical scheme described here is a dissipative scheme and therefore, we will show results with and without artificial viscosity. Von Neuman Richtmyer type viscous terms are used herein. If the equations (2.8) and (2.9) are written in the form:

$$\underline{w}_t + \underline{f}(\underline{w})_x = H(\underline{w}) \tag{3.7}$$

$$\text{where } \underline{w} = \begin{pmatrix} \rho \\ u \end{pmatrix}$$

then the artificial viscous term added to (3.7) is

$$\nu \frac{\partial}{\partial x}\left(\mid \rho_x \mid \frac{\partial \underline{w}}{\partial x} \right) \tag{3.8}$$

where $\nu = 0(1)$. We differenced this quantity according to the following formula.

$$\nu \frac{\partial}{\partial x}\left(\mid \rho_x \mid \frac{\partial \underline{w}}{\partial x} \right) \approx \frac{\nu}{\Delta x}\Big[\mid \rho_{j+1} - \rho_j \mid \left(\underline{w}_{j+1} - \underline{w}_j \right)$$

$$- \mid \rho_j - \rho_{j-1} \mid \left(\underline{w}_j - \underline{w}_{j-1} \right) \Big] \tag{3.9}$$

This is a second order formula. This formula is used in both stages of our scheme up to the boundary. The added viscosity terms tend to reduce the accuracy of the scheme. Nevertheless, it provided better results than other types viscosity models we tried and gave a sharper shock with reasonably accurate solutions in the smooth regions. We shall see this later in our comparison with the asymptotic method of reference 7.

4. Boundary Conditions.

In this section we consider some questions concerning boundary conditions. First, we need a nonreflective boundary condition at the exit section of the duct. Next we need boundary conditions appropriate to the numerical scheme. These are accomplished by obtaining characteristic variables for the system (2.4) and (2.5). We linearize this system to get

$$\underline{w}_t + A\underline{w}_x = 0 \tag{4.1}$$

where

$$A = \begin{pmatrix} u_s & \rho_s \\ \frac{c_s^2}{\rho_s} & u_s \end{pmatrix} \text{ and } \underline{w} = \begin{pmatrix} \rho \\ u \end{pmatrix}$$

The eigenvalues of this matrix are

$$\lambda_+ = u_s + c_s \text{ and } \lambda_- = u_s - c_s$$

We note that $u_s < c_s$ thus λ is strictly negative. The signs of these eigenvalues gives the characteristic directions of propagation flow. At x $= 0$, $\lambda_+ > 0$ gives the inflow direction and $\lambda_- < 0$ gives the outflow direction. Similarly at x $=$ L, $\lambda_+ > 0$ gives the outflow and λ_- inflow directions respectively. The matrix formed by the eigenvectors is

$$T = \begin{pmatrix} 1 & 1 \\ \frac{c_s}{\rho_s} & \frac{-c_s}{\rho_s} \end{pmatrix} \tag{4.2}$$

so that $T^{-1}AT$ is diagonal. The characteristic variables are then

$$\underline{v} = T^{-1}\underline{w} \tag{4.3}$$

If

$$\underline{v} = \begin{pmatrix} v_1 \\ v_2 \end{pmatrix}$$

then

$$v_1 = \frac{\rho}{\rho_s} + \frac{u}{c_s}$$
$$v_2 = \frac{\rho}{\rho_s} - \frac{u}{c_s} \tag{4.4}$$

Here v_1, v_2 corresponds to the eigenvalues λ_+ and λ_- , respectively. At x = L v_2 is the inflow variable. Setting $v_2 = 0$, i.e.

$$\frac{\rho}{\rho_s} - \frac{u}{c_s} = 0 \tag{4.5}$$

is exactly the nonreflective condition stated by the general form in (2.13). In linear acoustics this is known as the impedence condition.

For the numerical scheme it was found effective prescribing the boundary conditions in terms of these variables v_1 and v_2. At $x = 0$, v_2 is computed through an iteration. Let us call this value to be v_2^c . Thus

$$\frac{\rho}{\rho_s} - \frac{u}{c_s} = v_2^c \tag{4.6}$$

But u is prescribed at x=0.

$$u = f \tag{4.7}$$

Solving (4.7) and (4.6) for u and ρ we have

$$u = f; \quad \rho = \rho_s\left(v_2^c + \frac{f}{c_s}\right) \tag{4.8}$$

Similarly, at x = L, we compute v_1. This gives

$$\frac{\rho}{\rho_s} + \frac{u}{c_s} = v_1^c \tag{4.10}$$

We solve (4.5) and (4.10) to obtain the values of u and ρ at x = L. They are

$$\rho = \rho_s v_1^c/2$$
$$u = c_s v_1^c/2 \tag{4.11}$$

Together with these conditions the solutions were started at a state of rest and iterated over 6 periods to obtain the results discussed in the next section.

5. Discussion of results.

The procedures developed in the previous sections were applied to a particular geometry called a Crocco-Tsien duct. A detailed description of the contour of the duct is available in reference 6. This contour is designed in such a way that, the mean flow accelerates linearly to Mach number unity at the throat. In particular, for the examples given here the entry Mach number at the exit section was -.50 and at the throat -.90 ($=M_t$). Here the "minus" sign denotes the flow in the negative x direction.

Figure 1(a) shows a typical configuration of the duct. Figure 1(b) shows the area variation. This geometry has exit/throat ratio about 1.32, so that this area variation provides a gradual choking of the flow. In this case the Mach number distribution becomes as depicted in figure 2. With this area variation and Mach number distribution, the steady flow equations satisfied by ρ_s and u_s (equations 2.5 and 2.6) were solved explicitly (see also [4]).

As we discussed previously, the finite difference algorithm is compared with the asymptotic theory developed in reference 7. Since the typical nonlinear situation arises at higher sound pressure levels and Mach numbers approaching unity, in this theory a small peaturbation parameter was chosen as $(1- \mid M_t \mid)$, where M_t is the throat Mach number. Comparisons for a value for $M_t = -.90$ are given in figures 3 and 5 respectively. The strengths for an equivalent sound pressure source located at x=0 (figure

1a) are roughly 149 and 156dB, respectively. Corresponding to equation (2.12) they have the form

$$f(t) = A\cos t,$$

where A is the amplitude calculated according to the source strength. In both (149dB and 156dB) cases shocks were predicted in reference 7. In these figures the time history of the velocity over a period (2π) is given. The velocity is normalized by $(1- \mid M_t \mid)^2$ since the acoustic velocity is small in magnitude. Thus the actual value of the acoustic velocity is of the order 10^{-3} or less. This is exactly the reason a higher order accurate scheme was necessary. The solid lines in these figures are the numerical solution and the other (see figures 3 and 5) are the asymptotic solutions computed at x = 0.75L and at the exit x = L respectively. The finite difference calculations agree well with the asymptotic theory. The difference scheme we used itself is a dissipative scheme. We carried out the computations without artificial viscosity terms in the algorithm. For the case of 149dB source the results are shown in figure 7. The comparison is still good in the smooth regions. Results shown in figures 3 and 7 also validate the fact that the amount of added artificial viscosity did not affect the physics of the wave nature.

Finally, figures 4 and 6 show the overall sound pressure level (dB) in the duct. Figure 4 corresponds to the shock case of 149dB sound source. This is a very weak shock case. At the exit we see a 2dB sound pressure level reduction. Figure 6 shows the sound pressure level for a 156dB source. In this case we see a sound pressure level reduction about 5dB at the exit. These results show that the higher the sound source level one obtains

substantial sound reduction through loss of energy due to shocks.

Extension of this work in two dimensions is in progress by the authors. The results will be reported elsewhere.

Acknowledgements

The authors would like to acknowledge useful discussions had with Drs. A. Bayliss, M. E. Rose, E. Turkel. In particular hours of discussions with Dr. M. K. Myers.

References

1. Blackstock, D. T., "Connection Between the Fay and Fubini Solutions for Plane Waves of Finite Amplitude," Jour. of Acous. Soc. of Am, Vol. 39, No. 6 (1966), pp. 1019-1026.

2. Gottlieb, D. and Turkel, E., "Dissipative Two-Four Methods for Time Dependent Problems", Math. Comp., 30(1976), pp. 703-723.

3. Greatrix, F. B., "By-Pass Engine Noise", Trans., SAE, Vol. 69 (1961), pp. 312-324.

4. Hariharan, S. I. and Lester, H. D., "A Finite Difference Solution for the Propagation of Sound in Near Sonic Flows", NASA TM - 84663 (1983).

5. Jones, M. G, "An Experimental Investigation of Sound Attenuation in a High-Subsonic Mach Number Inlet", M. S. Thesis, The George Washington University (1982).

6. Myers, M. K. and Callegharí, A. J. "On the Singular Behvior of Linear Acoustic Theory in Near Sonic Duct Flows", J. of Sound and Vib., 51 (4) (1977), pp. 517-531.

7. Myers, M. K., "Shock Development in Sound Transmitted Through a Nearly Choked Flow," AIAA-81-2012.

8. Myers, M. K. and Callegharí, A. J., "Acoustic Shocks in Nearly Choked Flows", AIAA - 80 - 1019.

9. Nayfeh, A. H. Kelly, J. J. and Watson, L. T., "Nonlinear Propagation in Near Sonic Flows", AIAA - 80 - 0096.

10. Polyakova, "Plane Sound Waves of Finite Amplitude in a Moving Medium", Soviet Physics, Doklady, Vol. 6, No. 4 (1961).

11. Turkel, E., "On the Practical Use of High Order Methods for Hyperbolic Stystems". ICASE report No. 78-19 (1978).

12. Walkington, N. J. and Eversman, W., "Finite Difference Solutions to Shocked Acoustic Waves", AIAA - 83 - 0671.

VARIABLE AREA FLOW DUCT

COORDINATE GEOMETRY

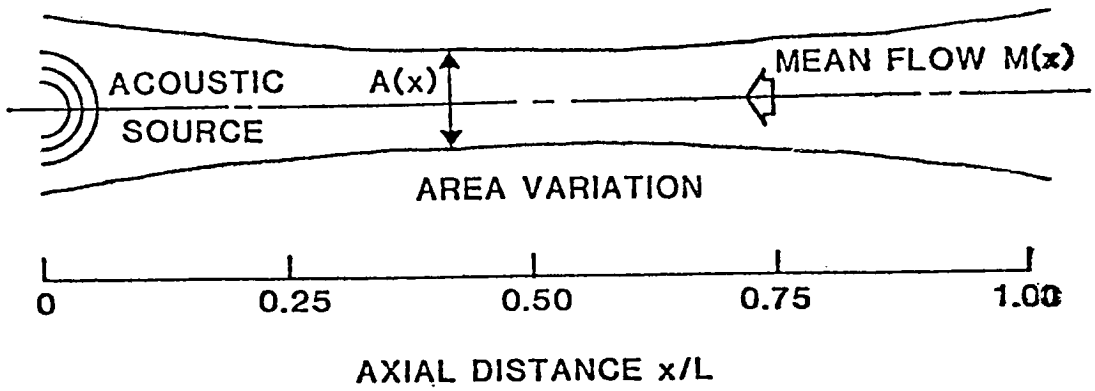

Figure 1(a)

VARIABLE AREA FLOW DUCT

AREA VARIATION

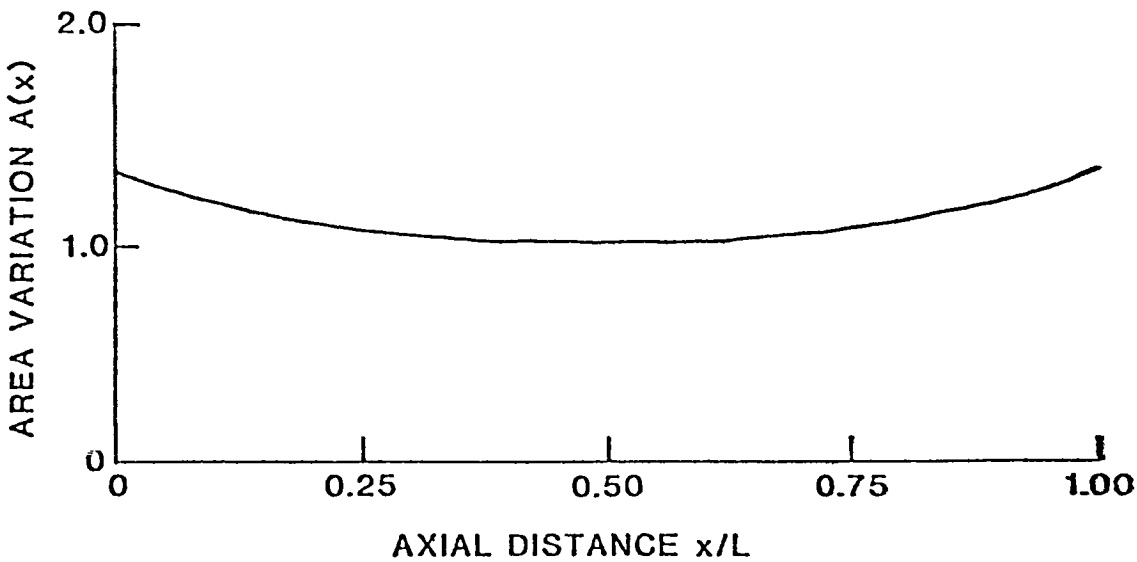

Figure 1(b)

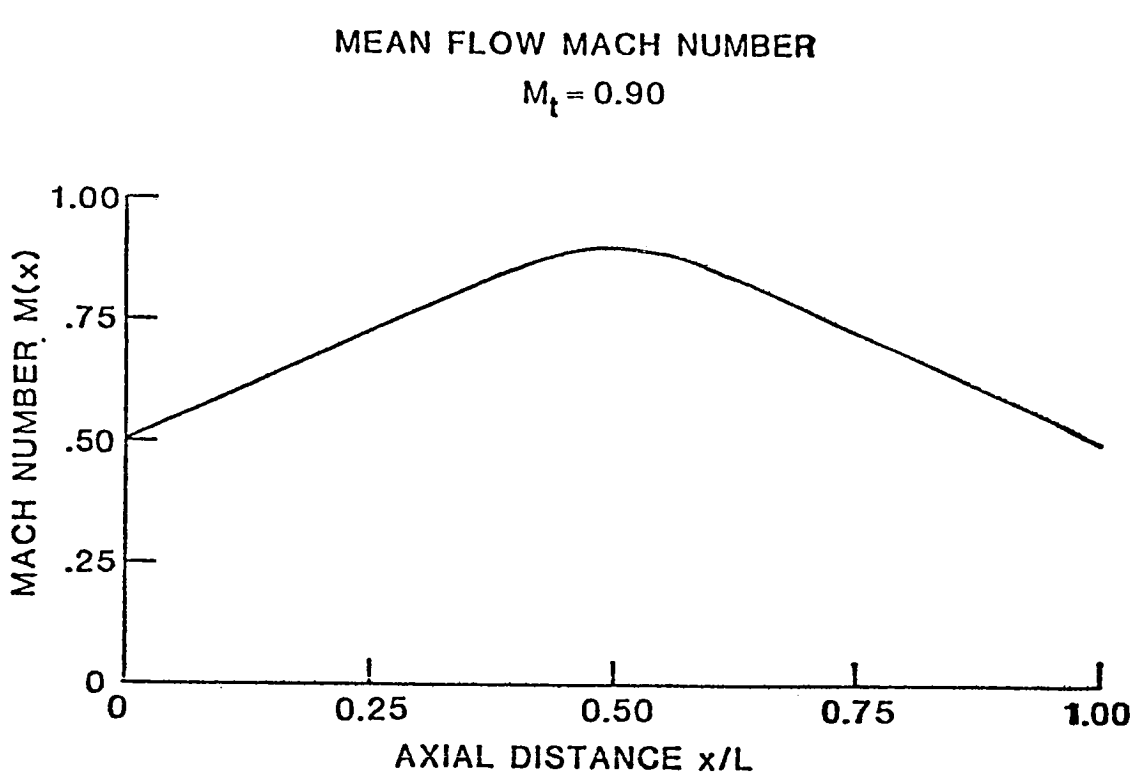

Figure 2

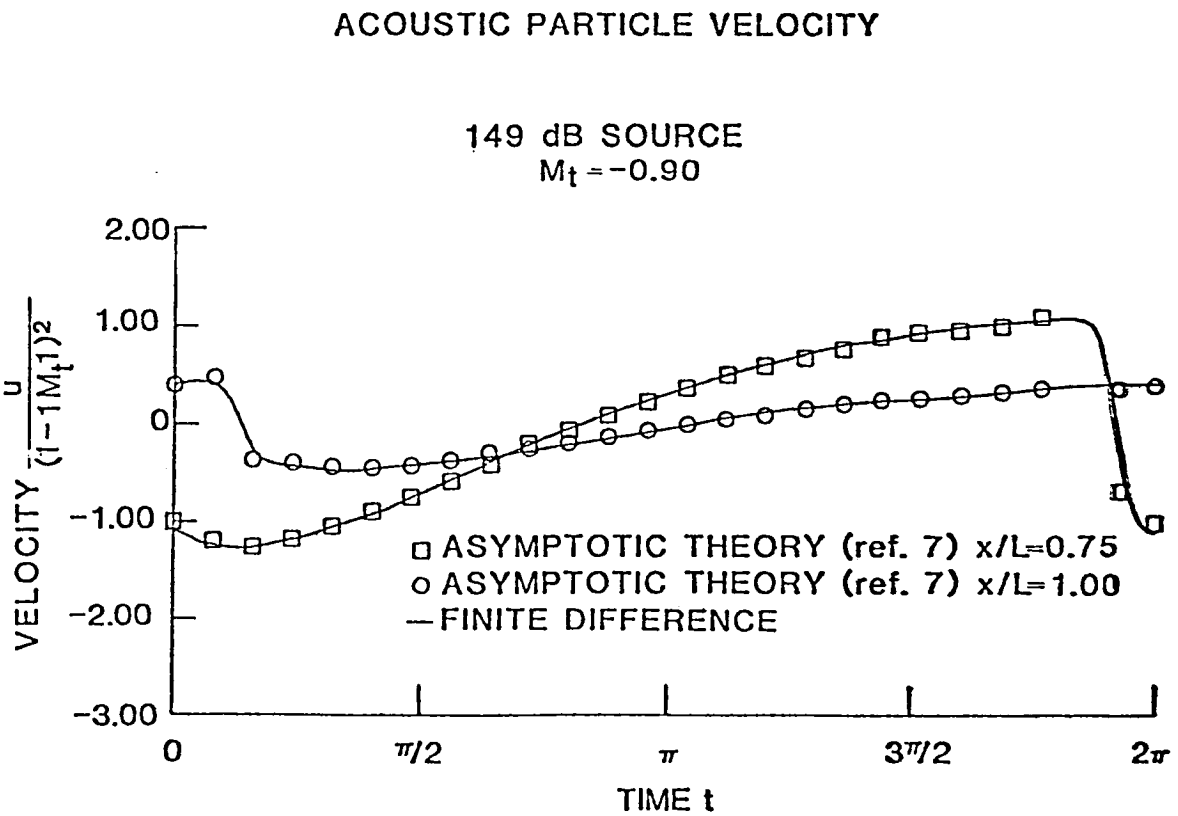

Figure 3

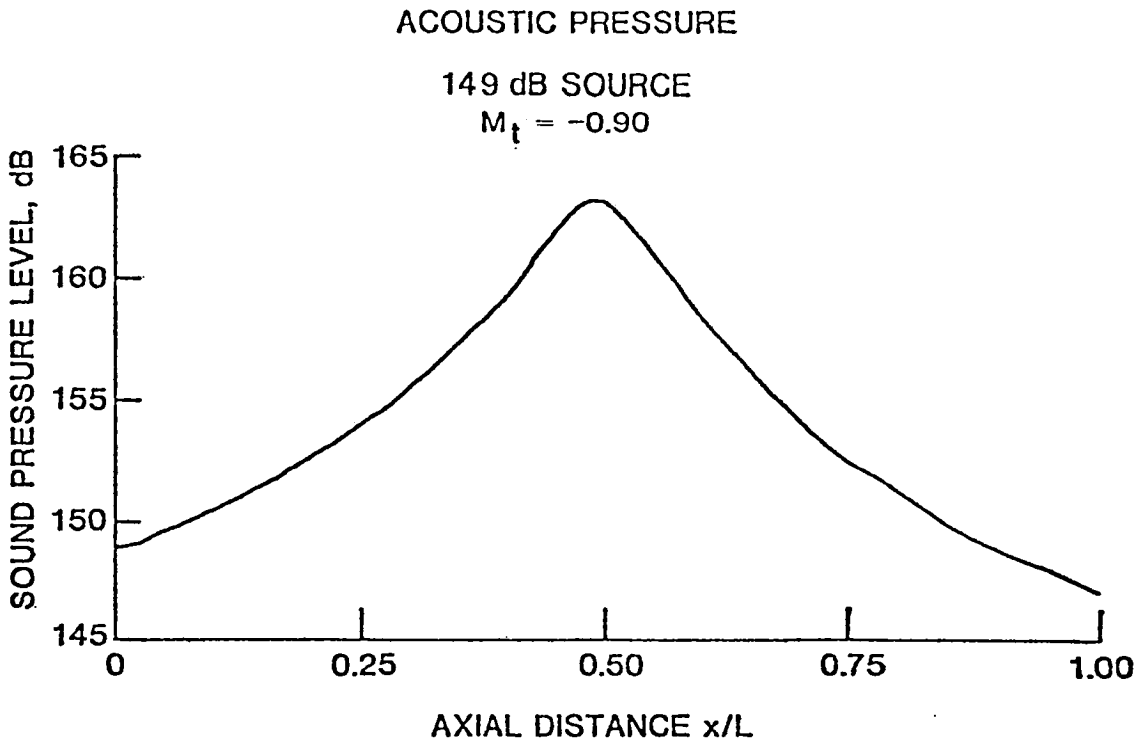

Figure 4

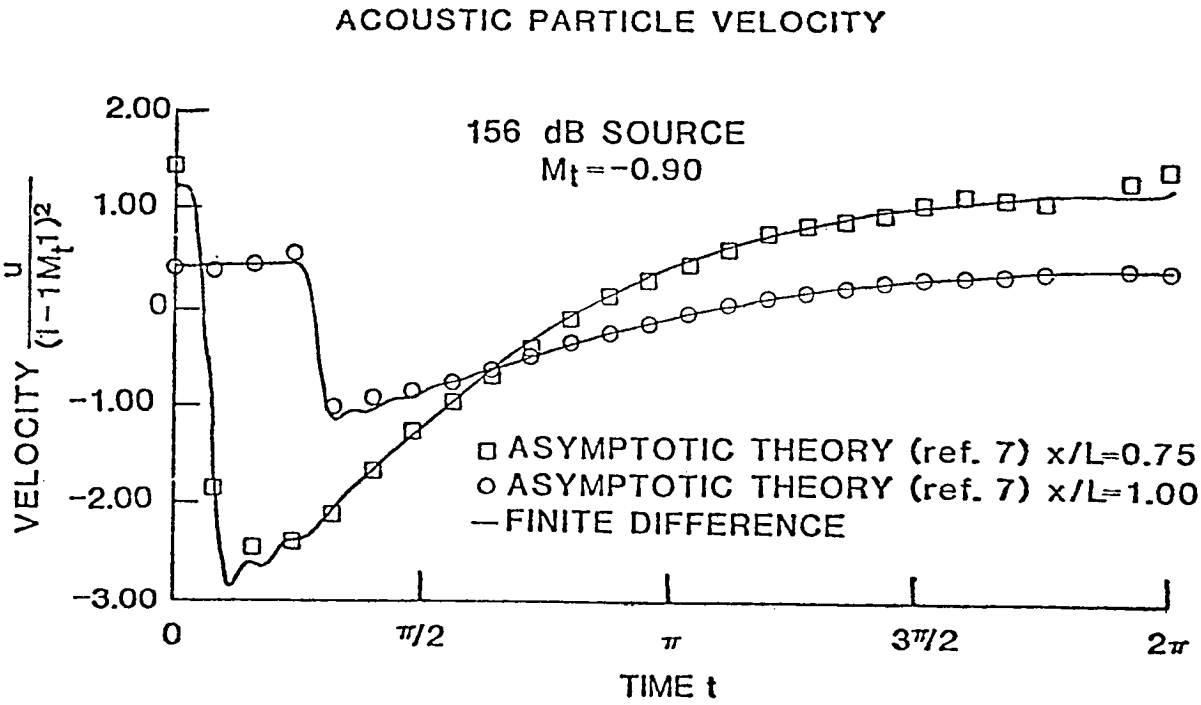

Figure 5

ACOUSTIC PRESSURE

156 dB SOURCE
$M_t = -0.90$

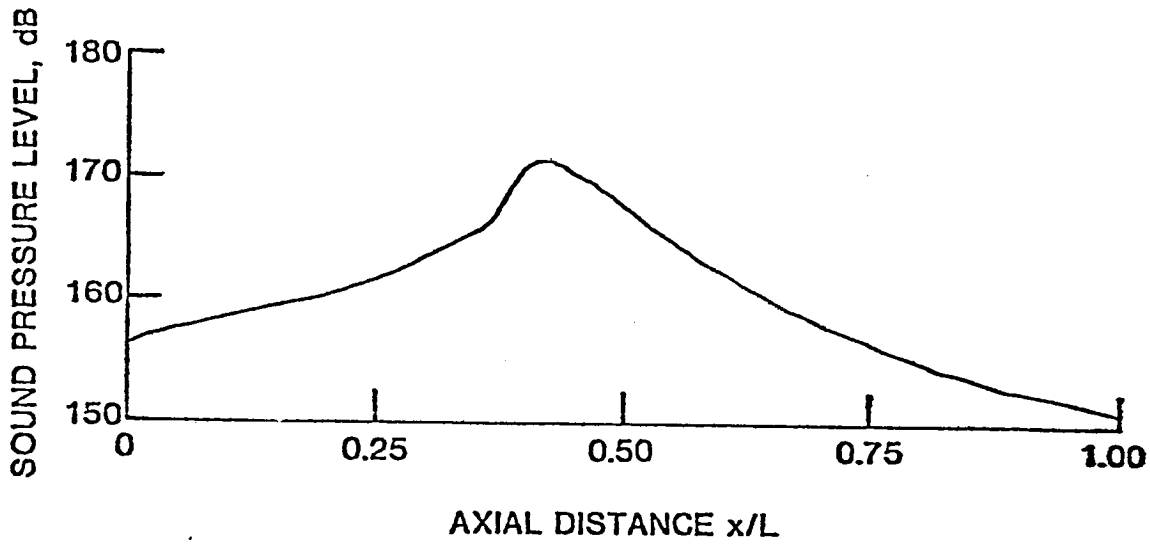

Figure 6

ACOUSTIC PARTICLE VELOCITY
WITHOUT ARTIFICIAL VISCOSITY

149 dB SOURCE
$M_t = -0.90$

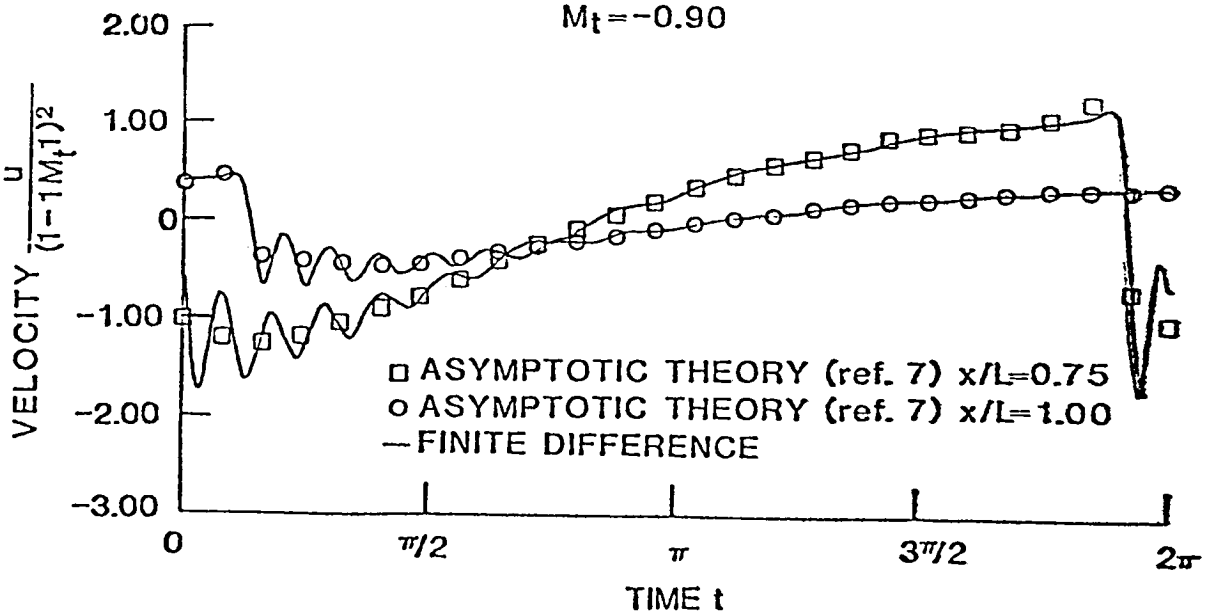

Figure 7

1. Report No.	2. Government Accession No.	3. Recipient's Catalog No.
NASA CR-172274		

4. Title and Subtitle	5. Report Date
Acoustic Shocks in a Variable Area Duct Containing Near Sonic Flows	December 1983
	6. Performing Organization Code
7. Author(s)	8. Performing Organization Report No.
S. I. Hariharan and Harold C. Lester	83-64
	10. Work Unit No.
9. Performing Organization Name and Address Institute for Computer Applications in Science and Engineering Mail Stop 132C, NASA Langley Research Center Hampton, VA 23665	11. Contract or Grant No. NAS1-17070, NAS1-17130
	13. Type of Report and Period Covered contractor report
12. Sponsoring Agency Name and Address National Aeronautics and Space Administration Washington, D.C. 20546	14. Sponsoring Agency Code

15. Supplementary Notes

Langley Technical Monitor: Robert H. Tolson
Final Report

16. Abstract

In this paper we consider acoustic shock waves in a variable area duct which contains near sonic flows. The problem we treat here is modeled after an aeroengine inlet. It is known experimentally that area variation of a duct and high Mach number mean flow can reduce acoustical energy yielding substantial noise reduction. One possible reason for this is acoustic shocks. We describe the use of an explicit numerical method which is very accurate and also captures shocks reasonably well. Comparisons of the results are made with an existing asymptotic theory for Mach numbers close to unity. When shock occurs reduction of sound pressure levels are shown by examples.

17. Key Words (Suggested by Author(s))	18. Distribution Statement
nonlinear acoustics shock waves finite differences characteristic boundary conditions	71 Acoustics Unclassified-Unlimited

19. Security Classif. (of this report)	20. Security Classif. (of this page)	21. No. of Pages	22. Price
Unclassified	Unclassified	20	A02

For sale by the National Technical Information Service, Springfield, Virginia 22161 NASA-Langley, 1984